Role of pH in a nitric oxide-dependent increase in cytosolic Cl⁻ in retinal amacrine cells

Emily McMains and Evanna Gleason
Department of Biological Sciences, Louisiana State University, Baton Rouge, Louisiana

McMains E, Gleason E. Role of pH in a nitric oxide-dependent increase in cytosolic Cl⁻ in retinal amacrine cells. *J Neurophysiol* 106: 641–651, 2011. First published May 18, 2011; doi:10.1152/jn.00057.2011.—Nitric oxide (NO) synthase-expressing neurons are found throughout the vertebrate retina. Previous work by our laboratory has shown that NO can transiently convert inhibitory GABAergic synapses onto cultured retinal amacrine cells into excitatory synapses by releasing Cl⁻ from an internal store in the postsynaptic cell. The mechanism underlying this Cl⁻ release is currently unknown. Because transport of Cl⁻ across internal membranes can be coupled to proton flux, we asked whether protons could be involved in the NO-dependent release of internal Cl⁻. Using pH imaging and whole cell voltage-clamp recording, we addressed the relationship between cytosolic pH and cytosolic Cl⁻ in cultured retinal amacrine cells. We found that NO reliably produces a transient decrease in cytosolic pH. A physiological link between cytosolic pH and cytosolic Cl⁻ was established by demonstrating that shifting cytosolic pH in the absence of NO altered cytosolic Cl⁻ concentrations. Strong buffering of cytosolic pH limited the ability of NO to increase cytosolic Cl⁻, suggesting that cytosolic acidification is involved in generating the NO-dependent elevation in cytosolic Cl⁻. Furthermore, disruption of internal proton gradients also reduced the effects of NO on cytosolic Cl⁻. Taken together, these results suggest a cytosolic environment where proton and Cl⁻ fluxes are coupled in a dynamic and physiologically meaningful way.

GABAergic signaling; postsynaptic; modulation

THE REGULATION of cytosolic Cl⁻ is likely to be important for the normal function of any cell type. However, it is especially relevant to the function of neurons because the distribution of Cl⁻ across the postsynaptic plasma membrane determines the weight and sign of GABAergic and glycinergic synaptic signaling. It is well established that key players in the regulation of cytosolic Cl⁻ are two plasma membrane Cl⁻ cotransporters: the K⁺-Cl⁻ cotransporter (KCC) and the Na⁺-K⁺-Cl⁻ cotransporter (NKCC). Furthermore, cytosolic Cl⁻ can also be regulated by Na⁺-dependent and Na⁺-independent Cl⁻/HCO₃⁻ exchangers (Farrant and Kaila 2007; Kim and Trussell 2009) and by Cl⁻-conducting ion channels (Foldy et al. 2010; Staley et al. 1995). We have identified another mechanism for regulating cytosolic Cl⁻ that involves a nitric oxide (NO)-dependent release of Cl⁻ from an as-yet-unidentified internal store (Hoffpauir et al. 2006). Although the store and transporter(s) involved are not known, there are several internal Cl⁻ transport mechanisms that are candidates. Currently, four classes of Cl⁻ channels/transporters can be localized to internal membranes (for a review, see Duran et al. 2010): anoctamins (Ca²⁺-dependent Cl⁻ channels), bestrophins

(Cl⁻ channels, possibly Ca²⁺ dependent), Cl⁻ intracellular channels (CLICs; Cl⁻ channels regulated by oxidation and pH), and internal Cl⁻ channels (CLCs; Cl⁻/H⁺ exchangers). This diversity of internal Cl⁻ transporters suggests that intracellular Cl⁻ gradients are both regulated and dynamic.

NO is a gaseous signaling molecule produced by cells expressing NO synthase (NOS), a Ca²⁺-sensitive enzyme that converts arginine into citrulline and NO. Subsets of all retinal cell types, including amacrine cells, express this enzyme and can presumably be stimulated to produce NO. NOS-expressing amacrine cells have recently been determined to respond to light stimuli with transient depolarization (Pang et al. 2010). There is evidence that NO can affect multiple cellular processes in the retina; however, relatively little is known about the effects of NO on signaling in the inner retina. NO has been shown to inhibit light responses from "on," "off," and "on/off" ganglion cells in the ferret retina (Wang et al. 2003). This inhibition was mimicked by blocking glycinergic signaling, suggesting the involvement of amacrine cells in this modulation. Conversely, pharmacological inhibition of NO production decreased inhibition onto ganglion cells (Nemargut and Wang 2009). However, ganglion cells in neuronal NOS (nNOS) knockout retinas required more light than wild-type cells to respond optimally, indicating that completely removing nNOS-stimulated NO production also decreases ganglion cell activity (Wang et al. 2007). Together, these findings indicate that in the inner retina, NO plays a complex role in shaping retinal output.

Previous work by our laboratory has demonstrated that NO induces a cGMP-independent increase in intracellular Cl⁻ resulting from the release of Cl⁻ from internal compartments. Importantly, this NO-dependent increase in cytosolic Cl⁻ concentration has been shown to be capable of transiently converting normally inhibitory GABAergic synapses into excitatory synapses (Hoffpauir et al. 2006). What is the source of the increased Cl⁻? Although their sensitivity to NO is relatively unexplored, acidic internal compartments containing high concentrations of Cl⁻ are found in most eukaryotic cell types. Organelles such as endosomes (early and late), lysosomes, and synaptic vesicles are regulated to have both a low luminal pH and high levels of Cl⁻ (Faundez and Hartzell 2004). The acidity of these compartments is vital to their cellular function. Low pH is maintained by the inward pumping activity of vacuolar (V-type) H⁺-ATPase (Mellman 1992). One function of endosomal Cl⁻ is to minimize the electrical gradient across the endosomal membrane so that the H⁺ pump can function optimally (Sonawane and Verkman 2003). The established relationship between endosomal pH and Cl⁻ com-

pelled us to ask whether pH changes are involved in the NO-dependent release of Cl^- from internal stores.

MATERIALS AND METHODS

Cultures. Retinal cultures were prepared as previously described (Hoffpauir and Gleason 2002). Briefly, retinas from 8-day-old chick embryos were dissected and separated from the pigment epithelium and vitreous humor. Retinal tissue was mechanically and enzymatically dissociated (0.125% trypsin) and plated on poly-L-ornithine-treated 35-mm culture dishes to achieve a final cell concentration of $\sim 1.25 \times 10^5$ cells/dish. For pH imaging, cells were plated onto acid-washed poly-L-ornithine-treated glass coverslips placed in culture dishes. One day after cells had been plated, the extracellular media were replaced with a Neurobasal and 1% B27 neuronal nutrient medium (Invitrogen, Carlsbad, CA). Cells were fed with this media every other day until the cultures were no longer viable for experimentation (10–12 days). All methods using animals in this study were approved by the Institutional Animal Care and Use Committee of Louisiana State University (Assurance No. A3612-01).

Electrophysiology. Electrophysiology experiments were performed on isolated amacrine cells after 6–14 days in culture. Amacrine cells were identified based on previously established morphological criteria (Gleason et al. 1993). Culture dishes were mounted on an Olympus IX70 inverted microscope with contrast optics. Whole cell voltage-clamp recordings were made using an Axopatch 1-D amplifier, Digidata 1322A data-acquisition board, and Clampex 9.2 software (Molecular Devices, Sunnyvale, CA). A reference Ag/AgCl pellet in 3 M KCl was connected to culture dishes via an agar bridge containing 3 M KCl. Patch electrodes were pulled from thick-walled borosilicate glass using a Flaming/Brown puller (Sutter Instruments, Novato, CA) set to pull electrodes with tip resistance values from 3 to 8 MΩ. All recordings were made at room temperature.

Ruptured patch internal solutions were supplemented with an ATP regeneration system containing 50 U/ml creatine phosphokinase, 1 mM ATP disodium, 3 mM ATP dipotassium, 20 mM creatine phosphate, and 2 mM GTP disodium. For perforated-patch recordings using gramicidin D, 10 mg/ml stocks were prepared in 100% ethanol,

stored in the refrigerator, and used that day. Gramicidin stocks were diluted to 10 µg/ml in internal solution. Data recorded from cells that did not reach a stable series resistance value after attaining a 1-GΩ seal were discarded. Recordings with high series resistance values (>100 MΩ) were also discarded. Voltage-ramp experiments were corrected for series resistance errors before leak current subtraction. All data were corrected for junction potential. Calculated junction potential values (Clampex 9.2) were as follows: Cs^+ internal/control external, -11.9 mV; Cs^+ internal/NH_4Cl external, -11.8 mV; Cs^+ internal/0 Na^+ external, -12.4 mV; and HEPES internal/control external, -11.1 mV. Data collected from gramicidin perforated-patch experiments were not corrected for liquid junction potential (Kim and Trussell 2007).

pH imaging. Changes in pH were monitored using 5-(and-6)-carboxy SNARF-1, acetoxymethyl ester, acetate (SNARF-1 AM; Invitrogen). Cells were loaded with dye (2 µM) for 1 h, washed several times with HBSS (Invitrogen), and placed in an open recording chamber (Warner Instruments, Hamden, CT). For all pH imaging experiments except for those shown in Fig. 1A, inset, a Leica TCS-SP2 spectral confocal microscope with a ×63 oil-immersion lens was used to visualize changes in SNARF-1 AM fluorescence. The dye was excited with the 543-nm laser line. Fluorescence intensity over time was measured at two nonoverlapping bands of emission wavelengths centered on 590 and 640 nm. An increase in fluorescence at the former wavelength and a decrease in the latter wavelength were consistent with cytosolic acidification, whereas an increase at 640 nm and a decrease at 590 nm were consistent with cytosolic alkalinization. For pH imaging experiments using NO donors (Fig. 1A, inset), SNARF-1 AM fluorescence was visualized on an Olympus IX-70 inverted microscope fitted with a SNARF filter set with a 534-nm excitation peak and dual emission filters centered at 590 and 640 nm. Imaging recordings were acquired using a Sensicam QE cooled charge-coupled device camera (Cooke, Romulus, MI) and Slidebook ratio software (Intelligent Imaging Innovations, Denver, CO). Cells were kept under constant perfusion with normal external solution between drug applications. Fluorescence intensity data were subsequently analyzed using Origin 7.5 software (OrginLab, Northhampton, MA). Data were obtained by taking the ratio of fluorescence intensity at 640 nm to

Fig. 1. Nitric oxide (NO) transiently acidifies retinal amacrine cells. *A*: data from an amacrine cell loaded with the ratiometric pH indicator dye SNARF-1 AM. The normalized ratio of SNARF-1 fluorescence intensity at 640 and 590 nm is shown. An NO-induced decrease in the 640-to-590-nm ratio indicates that NO transiently acidified the cell. An equal volume of acidic solution did not decrease cytosolic pH. *Inset*, ~30-s application of 500 µM S-nitroso-N-acetyl-D,L-penicillamine (SNAP) also acidified cultured amacrine cells. Data averaged from nine responding cells are shown. Slight, steady declines in pH over the duration of the recording were subtracted from these data. *B*: data from a different SNARF-1-loaded amacrine cell. Exposure to 25 mM NH_4Cl resulted in cytosolic alkalinization. *C*: amiloride (300 µM) reversibly decreased cytosolic pH. *D*: mean normalized 640-to-590-nm ratios from multiple cells showing that NO and amiloride decreased pH and that NH_4Cl increased cytosolic pH. ns, $P > 0.05$ (not significant). ***$P < 0.001$.
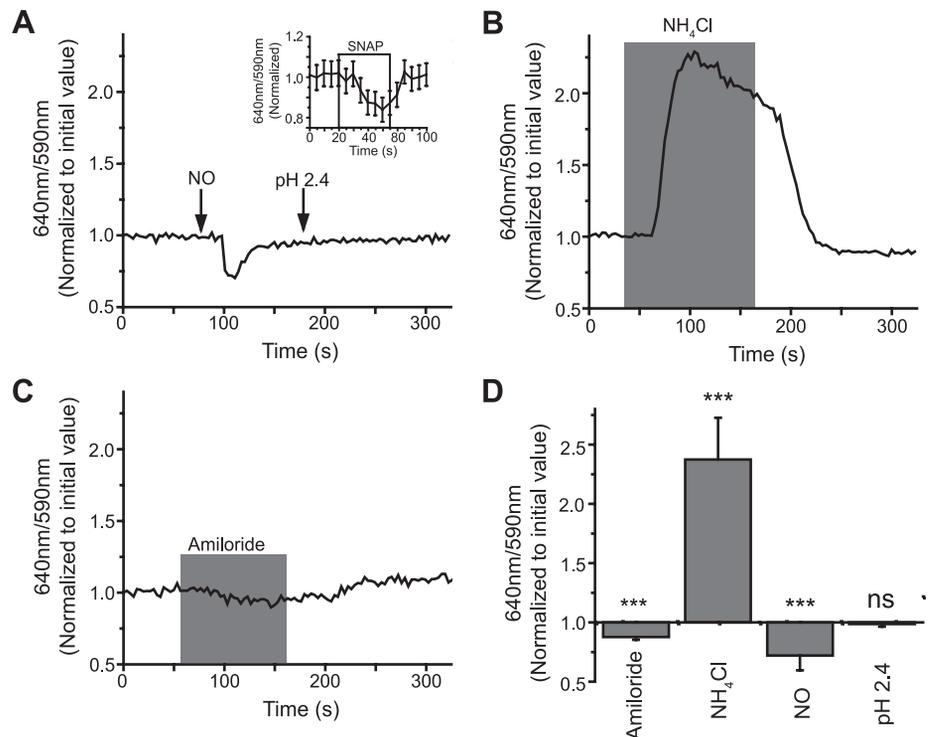
fluorescence intensity at 590 nm. Ratio values were normalized to the control data collected before the experimental manipulation.

Solutions. Unless otherwise indicated, reagents were obtained from Sigma-Aldrich (St. Louis, MO). Cells were continuously perfused with the external solution during recordings. For pH imaging experiments, the external recording solution contained NaCl (136.7 mM), KCl (5.3 mM), CaCl$_2$ (3 mM), MgCl$_2$ (410 μM), HEPES (10 mM), and glucose (5.6 mM). For electrophysiology experiments, the external recording solution contained NaCl (116.7 mM), KCl (5.3 mM), triethylammonium (TEA)-Cl (20 mM), CaCl$_2$ (3 mM), MgCl$_2$ (410 μM), HEPES (10 mM), and glucose (5.6 mM). For solutions containing 25 mM NH$_4$Cl, NH$_4$Cl was substituted for NaCl or TEA-Cl/NaCl. Both formulations gave similar results. For Na$^+$-free solutions, Na$^+$ was replaced with *N*-methyl-D-glucamine. The same Cl$^-$ concentration was maintained in all external recording solutions. All external solutions were corrected to a pH of 7.4. Rapid solution changes were achieved using a tri-barrel square glass assembly attached to a SF-77B Perfusion Fast Step (Warner Instruments, Hamden, CT) that could be controlled manually or by the computer software. When controlled manually, this apparatus achieved solution changes in 500 ms. For experiments requiring brief pulses of GABA, the software switched solutions in as little as 10 ms. In electrophysiology experiments, 300 nM TTX (Alomone Labs, Jerusalem, Israel) and 50 μM LaCl$_3$ were included in external solutions to block voltage-gated Na$^+$ and Ca^{2+} channels, respectively.

For ruptured patch recordings, the solution in the recording pipette contained cesium acetate (100 mM), CsCl (10 mM), CaCl$_2$ (0.1 mM), MgCl$_2$ (2 mM), HEPES (10 mM), and EGTA (1.1 mM) and the ATP regeneration system. For the 125 mM HEPES internal solution, the recording pipette contained HEPES (125 mM), CsCl (10 mM), CaCl$_2$ (0.1 mM), MgCl$_2$ (2 mM), and EGTA (1.1 mM), and pH and osmolarity were brought up to 7.4 and 240 mosM, respectively, with CsOH. For perforated-patch recordings, the ATP regeneration system was replaced with 20 mM cesium acetate. Bafilomycin was obtained from Enzo Life Sciences (Plymouth Meeting, PA). The NO donor *S*-nitroso-*N*-acetyl-D,L-penicillamine (SNAP) was obtained from Do-jindo Molecular Technologies (Rockville, MD) and was added directly to the external recording solution, which was then restored to pH 7.4.

NO solutions were prepared as previously described (Hoffpauir et al. 2006). Briefly, NO solutions were made by bubbling purified water with pure argon for 15 min and then by bubbling with pure NO that had been passed through a column of soda lime to filter out nitric dioxide for 15 min. These NO solutions were then tightly sealed, protected from light, and stored at 4°C until use. NO solution was injected directly into the perfusion line with a 50-μl glass Hamilton syringe. The typical injected volume was 30–50 μl. Previous measurements with injections of dye-containing solutions indicated that the delay between NO injection and exposure of cells to NO is ~2–3 s, the exposure time is limited to ~2–5 s, that most of the NO reaches the cells in the first 500 ms, and that the maximum NO concentration reaching the cells is <2 μM. The pH of undiluted NO solution exposed to air was ~2.5. Considering this to be the absolute lower limit for the pH of NO solution as it moves out of the perfusion system and on to the cells, we routinely injected pH 2.5 water (30–50 μl) into the perfusion lines to test for extracellular pH-dependent or low osmolarity effects. The only effect observed was a small change in holding current that was outward at −70 mV. Recordings during NO perfusion made with open (cell-free) electrodes showed no changes in current, indicating that NO application does not introduce junction potential errors. Furthermore, the NO effects described in this report were mainly observed after the bolus of NO solution would have cleared the environment of the recorded cells (>2–5 s; see above).

Statistical analysis. All quantitative comparisons of Cl$^-$ reversal potential (E_{Cl}) changes under different conditions were made using the same batch of NO solution within the same cells if possible. Comparisons were made between cells from the same culture day

when within-cell comparisons were not possible (different internal solutions, pretreatment). Data are presented as means ± SD. Differences between groups of data were assessed using Student's *t*-test. In the figures, one asterisk indicates $P < 0.05$, two asterisks indicate $P < 0.01$, three asterisks indicate $P < 0.001$, and ns indicates $P > 0.05$ (not significant). Exact *P* values are reported in the text.

RESULTS

Our previous work has shown that NO stimulates the transient release of Cl$^-$ from internal compartments in retinal amacrine cells (Hoffpauir et al. 2006). Possible sources for this Cl$^-$ are acidic, Cl$^-$-rich endosomal compartments. Because the movement of Cl$^-$ across internal membranes is often coupled to H$^+$ movement, we asked whether NO also affects cytosolic pH. Changes in cellular pH were monitored in cultured amacrine cells loaded with the ratiometric pH indicator dye SNARF-1 AM. NO induced a transient decrease in the ratio of 640/590-nm emission wavelengths of SNARF-1, consistent with NO-mediated cytosolic acidification (see MATERIALS AND METHODS; fold decrease in 640/590-nm intensity: 0.72 ± 0.12, $n = 20$; Fig. 1*A*) (Buckler and Vaughan-Jones 1990). An equal volume of low pH solution did not change cytosolic pH, indicating that the NO-induced acidification was NO dependent (fold change in 640/590-nm intensity: 0.99 ± 0.02, $n = 5$; Fig. 1*A*). Application of the NO donor SNAP also decreased the pH of some amacrine cells (35% of cells treated with 500 μM SNAP; Fig. 1*A*, *inset*).

Thus, NO has at least two effects on the cytosolic environment of amacrine cells. First, NO exposure leads to a transient elevation of cytosolic Cl$^-$ via release from an internal store (Hoffpauir et al. 2006). Here, we observed that NO also transiently reduces cytosolic pH. To determine whether these two outcomes are linked, we sought to manipulate cytosolic pH independently of NO. NH$_4$Cl exposure is frequently used to manipulate cytosolic pH (Boron and De Weer 1976). In the presence of 25 mM NH$_4$Cl, amacrine cells were consistently alkalinized (mean fold increase in 640/590-nm intensity: 2.37 ± 0.35, $n = 6$; Fig. 1, *B* and *D*) as NH$_3$ crossed the plasma membrane into the cytosol, leaving charged NH$_4^+$ and H$^+$ behind. Washing off NH$_4$Cl sometimes, but not always, produced an often irreversible acidification as the NH$_3$ gradient was reversed and the net flow of NH$_3$ was directed outward. Amiloride (300 μM), an inhibitor of Na$^+$/H$^+$ exchangers (NHEs), reversibly acidified amacrine cells (mean fold decrease in 640/590-nm intensity: 0.94 ± 0.06, $n = 5$; Fig. 1, *C* and *D*), indicating that NHEs are active at resting pH. These data demonstrate that NH$_4$Cl and amiloride can be used to reliably alkalinize and acidify (respectively) the amacrine cell cytosol. Interpretation of the effects of amiloride can be complicated by the fact that amiloride is known to inhibit other transport mechanisms (Frelin et al. 1988) (see DISCUSSION). As such, we attempted to use ethylisopropylamiloride (EIPA; 50 μM), an amiloride derivative more specific for NHEs. Unfortunately, EIPA produced chaotic changes in cytosolic pH, suggesting that its specificity may be different in avian neurons (data not shown).

Are the NO-induced acidification and the NO-dependent increase in cytosolic Cl$^-$ functionally linked? To address this question, we asked whether changing cytosolic pH would alter cytosolic Cl$^-$ concentrations as revealed by measuring the reversal potential of GABA-gated currents in amacrine cells.

These cells express GABA$_A$ receptors; therefore, GABA-gated currents are carried by Cl$^-$ (Hoffpauir et al. 2006). Previous work has established that changes in the reversal potential of GABA-gated currents in retinal amacrine cells primarily reflect changes in cytosolic Cl$^-$ concentrations (Hoffpauir et al. 2006). GABA$_A$ receptors are also permeable to bicarbonate (Bormann et al. 1987). To focus on the Cl$^-$ conductance such that the reversal potential of GABA $\sim E_{Cl}$, all experiments were conducted using nominally bicarbonate-free, HEPES-buffered solutions. Figure 2A shows our experimental protocol for measuring the E_{Cl} of retinal amacrine cells (see MATERIALS AND METHODS). Figure 2B shows a representative current-voltage relationship from a gramicidin perforated-patch recording generated using this experimental protocol. E_{Cl} was sampled every 10–20 s. Under these protocols, there was a slight decrease (leftward E_{Cl} shift) in internal Cl$^-$ over the course of each recording (see Figs. 3-5). Therefore, the net change, if any, created by the stimulus alone (GABA pulse delivered at −70 mV before and during voltage ramps from −90 to +50 mV) was outward Cl$^-$ movement. To minimize the impact of these small deviations on our data analyses, we were careful to compare the E_{Cl} in cells subjected to the same number of GABA stimuli. Nonetheless, it should be clear from the E_{Cl} over time plots shown in Figs. 3–5 that even though some variation in E_{Cl} occurred over the duration of the recordings, it was small compared with the effects of the experimental treatments.

Figure 3A shows data from a single amacrine cell in which the E_{Cl} was monitored over time under multiple conditions. The angled arrows indicate the time points from which differ-
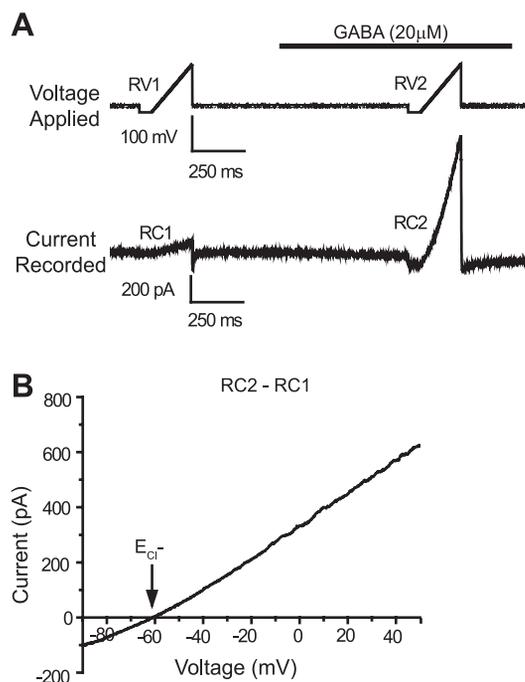

Fig. 2. Experimental protocol for measuring Cl$^-$ reversal potential (E_{Cl}). A: the *top* trace shows voltage protocol applied to cells. This paradigm was applied six times, once every 10 s. The *bottom* trace shows a typical recording produced by this protocol. RV1 and RV2, ramp voltage 1 and 2. B: gramicidin perforated-patch recording of a cell subjected to the voltage protocol in A. The first ramp current (RC1) was subtracted from the second ramp current (RC2; recorded in the presence of GABA) to give a direct measurement of E_{Cl}. Series resistance corrections were made before the subtraction.

ent current-voltage data were obtained. If the NO-dependent elevation of cytosolic Cl$^-$ and NO-mediated acidification are functionally linked, then we would predict that manipulating cytosolic pH with NH$_4$Cl and amiloride would alter internal Cl$^-$ levels in the absence of NO. In the ruptured patch configuration, 2-min applications of the alkalinizing agent NH$_4$Cl shifted the E_{Cl} of an amacrine cell in the negative direction (Fig. 3A,i), indicating that a basic cellular environment resulted in a significant decrease in internal Cl$^-$ (control mean E_{Cl}: −58.9 ± 3.8 mV and NH$_4$Cl mean E_{Cl}: −61.8 ± 3.4 mV, P = 0.0007, n = 6). In contrast, 300 μM amiloride, which acidifies cytosolic pH, shifted the E_{Cl} more positively (Fig. 3A,ii), indicating a significant increase in cytosolic Cl$^-$ under acidic cytosolic conditions (mean E_{Cl}: −54.00 ± 2.0mV, P = 0.0007, n = 5). The decrease in the slope of the current in amiloride (Fig. 3A,ii) was most likely due to a direct inhibition of GABA$_A$ receptors (Fisher 2002). Figure 3, B and C, shows that cytosolic alkalinization shifted the E_{Cl} in the negative direction and acidification shifted the E_{Cl} in the positive direction in each cell recorded.

Cells were also exposed to NO under control, alkalinizing, and acidifying conditions to determine whether the pH state of the cytosol would alter the NO-dependent shift in E_{Cl}. As shown for the cell in Fig. 3A, NO shifted the E_{Cl} in the positive direction, indicating the occurrence of the NO-dependent increase in cytosolic Cl$^-$ that we have previously demonstrated (Hoffpauir et al. 2006). Application of NO under basic cytosolic conditions demonstrated a significant decrease in the NO-induced E_{Cl} shift (Mean NH$_4$Cl NO E_{Cl} shift: 14.2 ± 10.4 mV and control shift: 34.9 ± 15.9 mV, n = 6, P = 0.02). In the same cells, cytosolic acidification with amiloride did not significantly alter NO-induced shifts in the E_{Cl} (mean E_{Cl} shift: 41.0 ± 4.8 mV, n = 6, P = 0.46). These data suggest that reducing the availability of H$^+$ in the cytosol limits the ability of NO to increase cytosolic Cl$^-$.

Because of concerns about the specificity of amiloride, and our inabililty to use EIPA in this preparation, we did similar experiments in the absence of extracellular Na$^+$ as an alternative way to inhibit the function of plasma membrane NHEs (Fig. 4). Removal of extracellular Na$^+$ will inhibit all plasma membrane Na$^+$-dependent transport mechanisms, not just the NHE, most notably NKCC, which normally functions to transport Cl$^-$ into cells. Under the conditions of these experiments (see DISCUSSION), however, the effects of 0 Na$^+$ were similar to amiloride in that 0 Na$^+$ produced an elevation in cytosolic Cl$^-$, as indicated by the consistent rightward shift in the E_{Cl} (mean control E_{Cl}: −63.3 ± 1.7 mV and mean 0 Na$^+$ E_{Cl}: −58.8 ± 2.1 mV, P = 0.002, n = 5; Fig. 4, C and D), the opposite result of what would be expected if the effects of 0 Na$^+$ were primarily due to blockade of ongoing NKCC activity.

The previous experiments were conducted in the ruptured-patch configuration. To determine whether the shifts in the E_{Cl} were observable in a more physiological internal Cl$^-$ environment, we repeated the experiments shown in Fig. 3A,i and ii, in the gramicidin perforated-patch recording configuration, where cytosolic Cl$^-$ is undisturbed by Cl$^-$ in the pipette solution. As in the ruptured-patch experiments, cytosolic alkalinization significantly decreased internal Cl$^-$ concentrations, whereas cytosolic acidification significantly increased internal Cl$^-$ concentrations (from mean control E_{Cl}: −60.0 ± 5.8 mV to mean NH$_4$Cl E_{Cl}: −64.3 ± 4.6 mV, P = 0.013, n = 5, and from
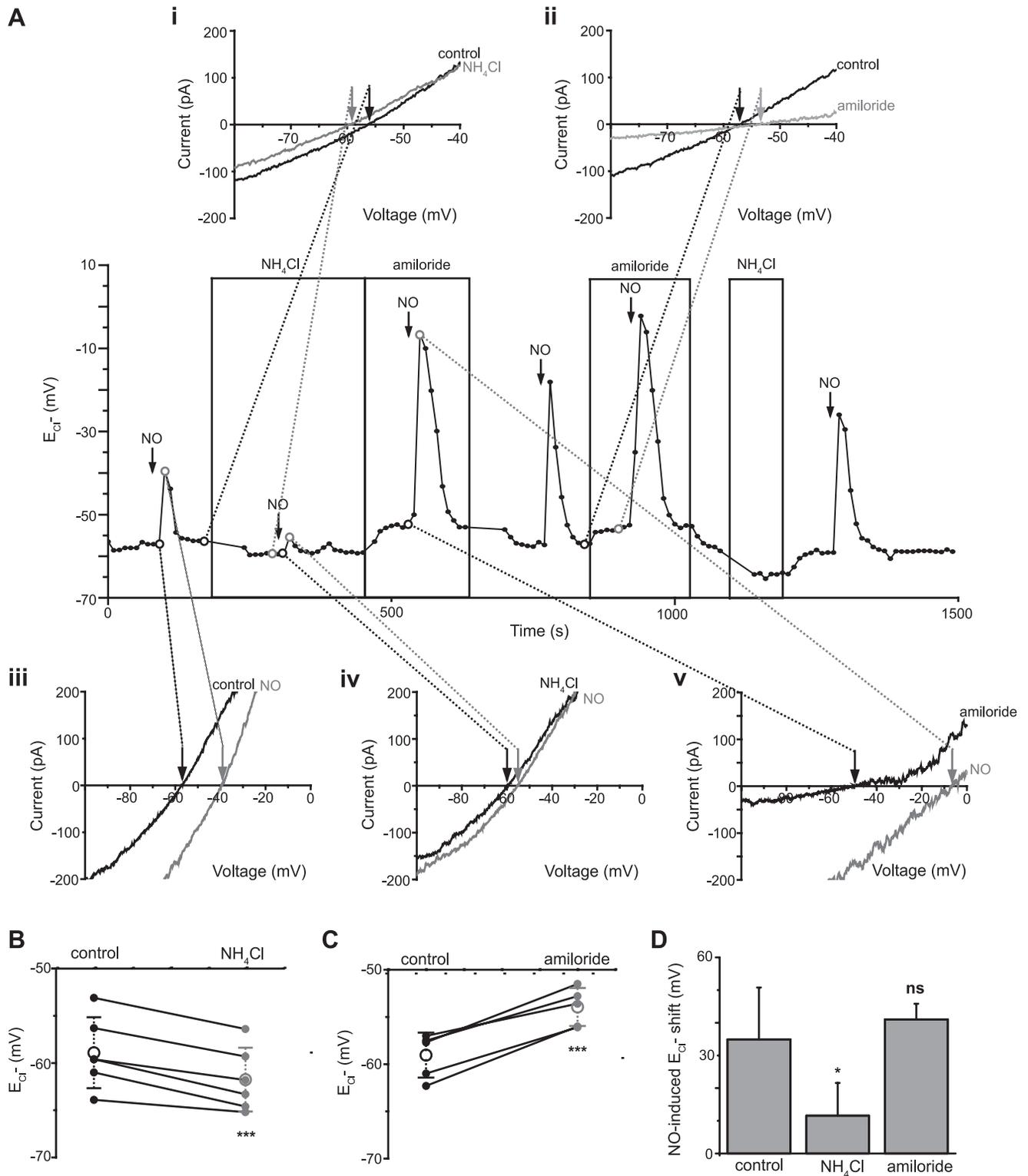
Fig. 3. Changing cytsolic pH changes cytosolic Cl^- concentrations. *A*, *middle*: changes in the E_{Cl} over time in a ruptured-patch voltage-clamp recording of a cultured amacrine cell. The large open circles correspond to E_{Cl} values measured from the leak-subtracted GABA currents shown in *i*–*v*. *i*, GABA currents recorded at resting intracellular pH (black) and after 2 min of alkalinization with 25 mM NH_4Cl (gray) showing that a rise in cytosolic pH induced a negative shift in E_{Cl}. *ii*, Amiloride (300 μM, gray trace) shifted the E_{Cl} to a more positive value in the same cell. *iii*, NO shifted the E_{Cl} ~20 mV in the positive direction under control conditions. *iv*, Alkalinization with NH_4Cl decreased the amplitude of the NO-induced E_{Cl} shift. *v*, The NO-induced shift in E_{Cl} in amiloride was larger (~50 mV) than the control in this cell. *B*: mean E_{Cl} (large open circles) in the presence of NH_4Cl (gray circles) was significantly more negative. *C*: mean E_{Cl} in the presence of amiloride (gray circles) was significantly more positive. Note that although there was variability in the E_{Cl} from cell to cell, for all cells tested, NH_4Cl and amiloride made E_{Cl} more negative and more positive, respectively. *D*: mean NO-induced E_{Cl} shifts demonstrating that NH_4Cl significantly decreased the amplitude of NO responses but that acidification with amiloride did not significantly alter NO responses. $*P < 0.05$; $***P < 0.001$; ns, $P > 0.05$.
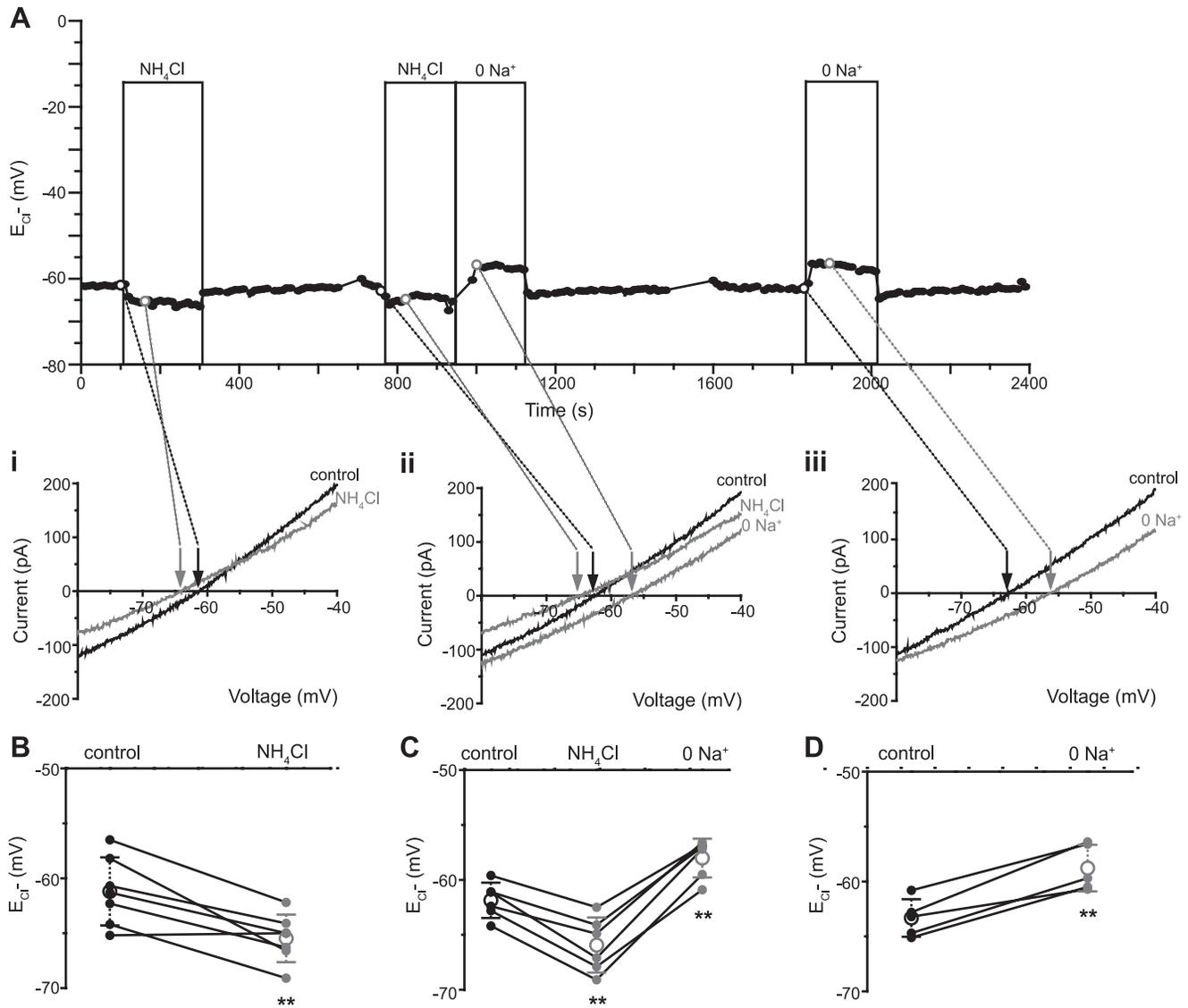
Fig. 4. Removal of extracellular Na^+ increases cytosolic Cl^- under recording conditions that minimize the contribution of the K^+-Cl^- cotransporter. *A*: changes in E_{Cl} over time and in the presence of NH_4Cl (25 mM) or 0 Na^+ external in an amacrine cell. *i*, NH_4Cl shifted E_{Cl} to the left. *ii*, Subsequent treatment with NH_4Cl also resulted in a negative shift in E_{Cl} and immediately switching to a Na^+-free external recording solution resulted in a positive shift in E_{Cl} with respect to control values. *iii*, Removal of external Na^+ alone positively shifted E_{Cl}. *B–D*: mean changes in E_{Cl} in the presence and absence of NH_4Cl and extracellular Na^+ revealed that alkalinization with NH_4Cl decreased internal Cl^- and acidification with 0 Na^+ external increased internal Cl^-. **$P < 0.01$.

-60.9 ± 4.1 to -56.3 ± 3.5 mV in amiloride, $P = 0.005$, $n = 6$; Fig. 5, *A–C*). These data further support the finding that changing the pH of retinal amacrine cells is sufficient to alter cytosolic Cl^- levels.

Thus far, these results have demonstrated a functional link between changes in cytosolic pH and changes in cytosolic Cl^-. To further explore the mechanism underlying the NO-dependent increase in cytosolic Cl^-, we asked whether NO-induced acidification is required for the NO-dependent increase in cytosolic Cl^-. To address this question, we compared measurements of NO-induced E_{Cl} shifts from amacrine cells with our standard concentration of HEPES buffer (10 mM) in the recording pipette to those from cells with a high concentration of HEPES (125 mM, pH corrected to 7.4 as in control) in the internal recording solution. Whole cell, leak-subtracted GABA-gated currents recorded during voltage ramps revealed that strong pH buffering limits the ability of NO to shift the E_{Cl}

to a more positive value (mean 10 mM HEPES E_{Cl} shift: 31.5 ± 9.5mV, $n = 10$, and 125 mM HEPES shift: 13.9 ± 9.5 mV, $n = 10$, $P = 0.0006$; Fig. 6). This result implies that NO-induced acidification contributes to the NO-mediated increase in cytosolic Cl^- levels.

The acidification of internal compartments is dependent on the activity of V-type H^+-ATPase. Cl^- is transported into these compartments to counteract the voltage gradient caused by the activity of vesicular H^+ pumps. This observation led us to hypothesize that NO increases internal Cl^- by changing the pH gradient across internal membranes and thereby inhibiting or reversing the direction of Cl^- movement across endosomal membranes. The protonophore FCCP allows H^+ to move down electrochemical gradients. Although FCCP is typically used to collapse the H^+ gradient across the inner mitochondrial membrane, other transmembrane H^+ gradients could also be affected. To assess the dependence of the NO-induced increase
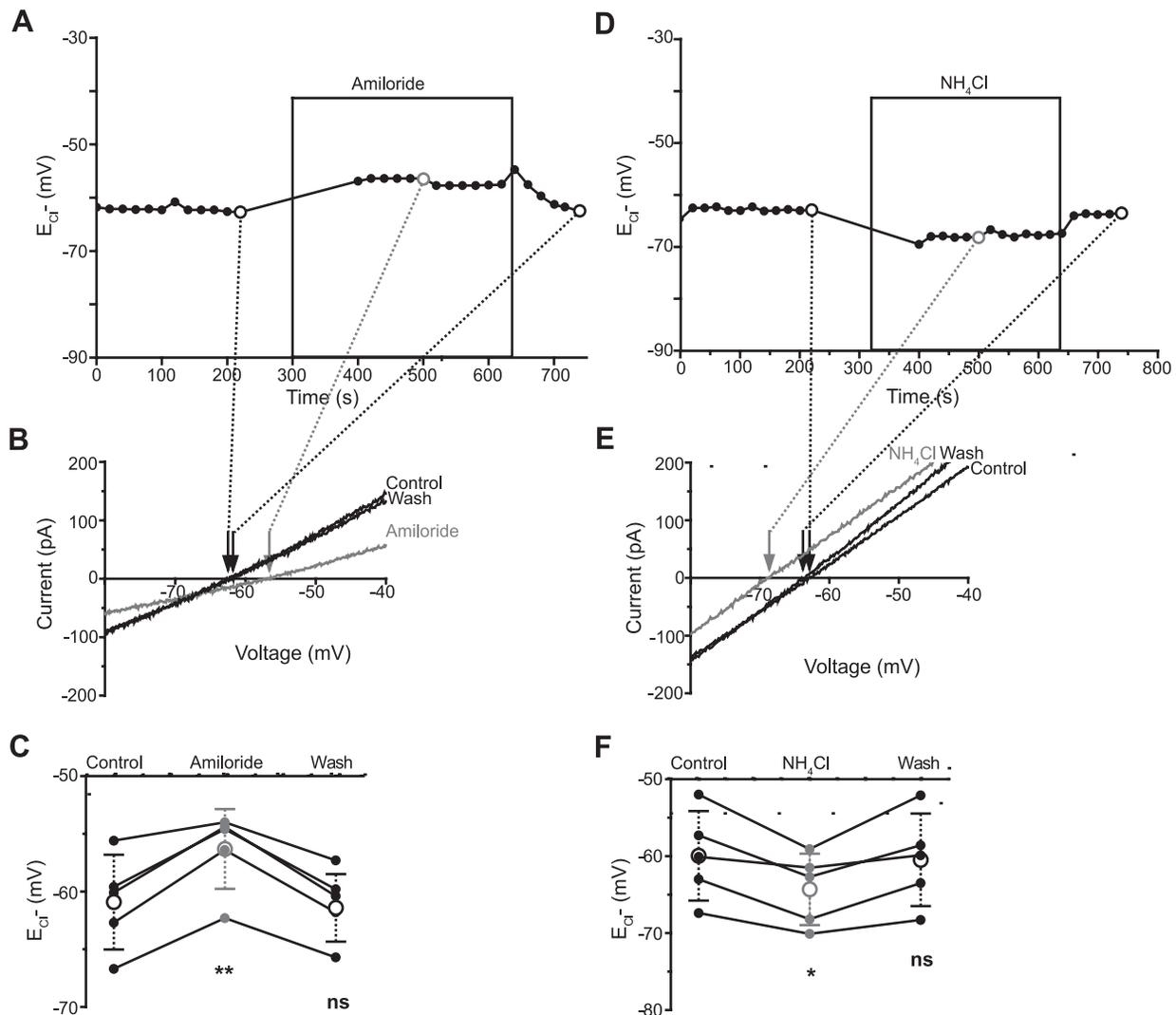
Fig. 5. Altering cytosolic pH changes intracellular Cl^- concentrations in gramicidin patch recordings. *A*: E_{Cl} values recorded over time in the presence and absence of amiloride. *B*: leak subtracted GABA-gated currents before (black trace), during (gray trace), and after (black trace) exposure to amiloride (300 μM). Amiloride treatment reversibly shifted E_{Cl} in the positive direction. *C*: mean E_{Cl} values in the presence and absence of amiloride are represented by large open circles. Amiloride increased internal Cl^- in every cell tested (small solid circles). *D*: E_{Cl} over time in a different amacrine cell. *E*: NH_4Cl alkalinization shifted E_{Cl} in the negative direction. *F*: mean NH_4Cl-induced changes in E_{Cl} were statistically significant, indicating that alkalinization lowered internal Cl^-. *$P < 0.05$; **$P < 0.01$; ns, $P > 0.05$.

in cytosolic Cl^- levels on internal H^+ gradients, we recorded NO-induced E_{Cl} shifts in amacrine cells in the presence and absence of FCCP. Cells were exposed to FCCP (1 μM) for 1–2 min, a concentration and application time known to disrupt the voltage-dependent activity of the mitochondrial Ca^{2+} uniporter but to not cause ATP depletion in amacrine cells (Medler and Gleason 2002). Treatment with FCCP significantly decreased NO-induced internal Cl^- release (mean E_{Cl} shifts for control: 62.5 $\pm$ 13.4 mV and for FCCP: 47.2 $\pm$ 19.9 mV, $n = 6$, $P = 0.014$; Fig. 7, *A–C*). To examine further the relationship between internal H^+ gradients and NO-mediated cytosolic Cl^- elevation, amacrine cells were also pretreated with the specific V-type H^+-ATPase inhibitor bafilomycin A1 (1 μM, 2 h) (Bowman et al. 1988). Bafilomycin treatment also significantly suppressed NO-induced E_{Cl} shifts (mean E_{Cl} shifts for control: 38.1 $\pm$ 5.0 mV and for bafilomycin: 29.0 $\pm$ 3.1, $n = 5$, $P = 0.008$; Fig. 7, *D–F*). Neither bafilomycin nor FCCP significantly altered E_{Cl} on their own (data not shown), indicating that plasma membrane Cl^- transport mechanisms are able to

manage cytosolic Cl^- under these conditions. Thus, the steepness of H^+ gradients across intracellular membranes is likely a factor in the ability of NO to elevate internal Cl^- concentrations in retinal amacrine cells.

DISCUSSION

These results show that in amacrine cells, cytosolic pH and cytosolic Cl^- concentration are functionally linked. We also show that the NO-dependent release of internal Cl^- relies in part on a change in cytosolic pH. Furthermore, we provided evidence that the NO-dependent release of internal Cl^- in these cells is influenced by the maintenance of internal H^+ gradients.

NO-, amiloride-, and NH_4Cl-dependent pH changes (as reported by normalized fluorescence intensity measurements) were of a similar order of magnitude. However, NO-dependent changes in internal Cl^- were, on average, ~10-fold larger than those caused by treatment with amiloride, 0 Na^+, or NH_4Cl.
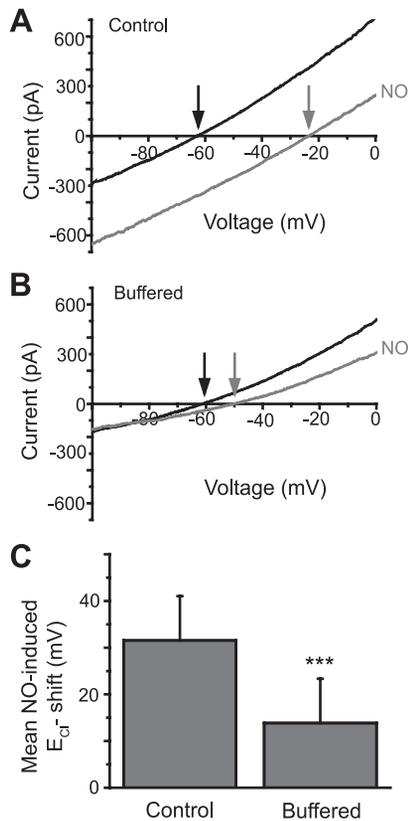
Fig. 6. Buffering internal pH inhibits the NO-induced internal Cl^- elevation. *A*: NO shifted E_{Cl} in an amacrine cell in the positive direction under control (10 mM HEPES) conditions. *B*: whole cell voltage-clamp recording of GABA currents before (black trace) and after (gray trace) NO in a cell containing a high (125 mM) concentration of HEPES buffer. The NO-induced E_{Cl} shift was decreased with respect to control (*A*). *C*: statistical comparison between NO-induced E_{Cl} shifts in control (10 mM HEPES) and buffered (125 mM HEPES) retinal amacrine cells demonstrating that cytosolic pH buffering inhibited the NO-dependent release of Cl^-. ***$P < 0.001$.

Furthermore, H^+ gradient inhibitors and increased intracellular buffering only partially inhibited the NO-mediated cytosolic Cl^- elevation. Although some of the limited inhibition may be due to incomplete dissolution of H^+ gradients by FCCP and bafilomycin and incomplete control of intracellular H^+ buffering by high concentrations of HEPES, it also seems likely that NO-mediated changes in pH direct only a part of NO-induced internal Cl^- release and that additional pH-independent mechanisms exist.

Internal Cl^- concentration is dependent on the relative activity levels of the full complement of Cl^- transport mechanisms expressed in different cell types. For example, a recent study of fast spiking cartwheel cells in the dorsal cochlear nucleus showed that activity-dependent acidification leads to a decrease in cytosolic Cl^-. However, complete removal of intracellular bicarbonate or blockade of bicarbonate transport not only inhibited this acidification-mediated cytosolic Cl^- reduction but reversed it, revealing an activity-dependent positive shift in the reversal potential for glycine (Kim and Trussell 2009). We found that the NO-dependent acidification of the cytosol drives an increase in cytsolic Cl^-. The apparent conflict between these two reports, however, may arise from differences in experimental conditions or from a different complement of transport mechanisms in cells with two very different levels of spiking activity. A relationship between the

active complement of transport mechanisms and normal activity levels has been established for two types of basket cells in the hippocampus. The basket cell type with fast spiking activity expressed a plasma membrane Cl^- channel (CLC2) that functioned to maintain a normal internal Cl^- concentration during strong $GABA_A$ receptor activity. This mechanism was either not used or not expressed in the slow spiking basket cells (Földy et al. 2010). Although amacrine cells are capable of producing action potentials, they do not normally undergo repetitive spiking like cartwheel cells. Significantly, it has been shown that NOS-positive amacrine cells in the mouse retina respond to light stimuli with transient depolarizations rather than spiking (Pang 2010).

Recording conditions can also alter the complement of active transport mechanisms. Previous work from our group has shown that in gramicidin recordings in the presence of internal K^+ (150 mM), removal of Na^+ from the bath solution decreased internal Cl^-, consistent with an inhibition of inward Cl^- movement by NKCC, leaving KCC to dominate the distribution of Cl^- across the plasma membrane (Hoffpauir et al. 2006). In the present study, we used internal solutions where K^+ was replaced with Cs^+ to eliminate the large outward K^+ currents that could compromise our accurate determination of E_{Cl}. Another consequence of this ion replacement is that Cs^+ attenuates the activity of KCC (Williams and Payne 2004). Under this condition of limited KCC activity, the removal of external Na^+ presumably inhibited the activity of both NKCC and NHE. The observed increase in Cl^- under these recording conditions are consistent with the dominant effect being inhibition of Na^+/H^+ exchange and an acidification-dependent cytosolic Cl^- elevation. It is important to note, however, that the NO-dependent shift in E_{Cl} persists in internal K^+ (rather than Cs^+), demonstrating that the underlying mechanism is not dependent on impaired KCC function (Hoffpauir et al. 2006).

NO and acidification. Although this is the first study to connect NO with changes in both pH and cytosolic Cl^-, NO-induced intracellular acidification has been previously reported. In the rat cerebellum, spreading depression and intracellular acidification are enhanced by NO donors and diminished by NOS inhibitors (Chen et al. 2001). In cultured hippocampal neurons, NO exposure induces a cytosolic acidification, which then activates the acid-sensitive endonucleases responsible for mediating programmed cell death (Vincent et al. 1999). NO-induced acidification is not limited to neuronal cells. NO acidifies cardiac myocytes by blocking NHE via a cGMP-dependent mechanism (Ito et al. 1997). Finally, NO has been shown to inhibit H^+-ATPase activity in reconstituted clathrin-coated vesicles (Forgac 1999). Thus, intracellular pH changes mediated by NO have been implicated in a diverse number of cellular processes and second messenger pathways.

Other mechanisms are known to stimulate cytosolic acidification in neurons. Many kinds of depolarizing stimuli lead to Ca^{2+}-dependent decreases in cytosolic pH in a number of different cell types, usually through the activation of plasma membrane Ca^{2+}-ATPase, which removes Ca^{2+} loads in exchange for an influx of H^+ (for a review, see Chesler 2003). In the retina, glutamate receptor activation acidifies horizontal cells through an unknown mechanism (Dixon et al. 1993; Trenholm and Baldridge 2010). Interestingly, in cultured ama-
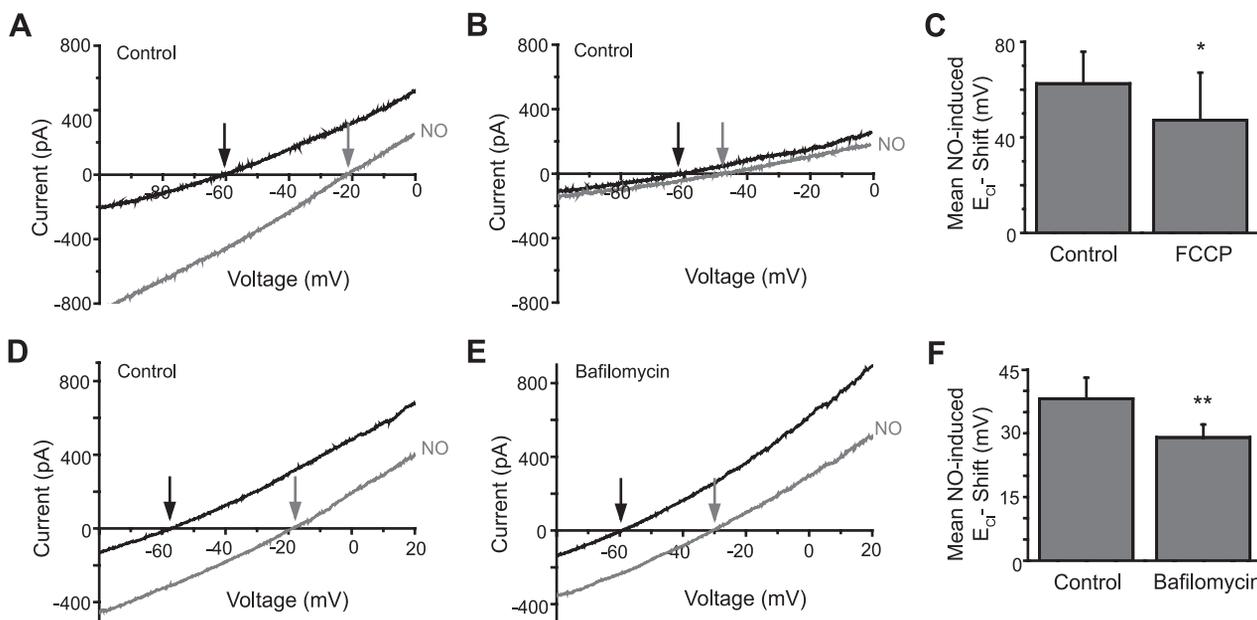
Fig. 7. Disruption of H^+ gradients decreases NO-induced cytosolic Cl^- elevation. *A*: whole cell voltage-clamp recording of NO-induced shift in E_{Cl}. *B*: in the same cell, treatment with FCCP decreased the amplitude of the NO-dependent shift. *C*: dissipation of internal pH gradients with FCCP significantly decreased the amplitude of NO-induced changes in E_{Cl}. *D*: NO shifted E_{Cl} in a control retinal amacrine cell. *E*: in a different amacrine cell, 2-h treatment with bafilomycin decreased the NO-induced E_{Cl} shift relative to control cells recorded on the same day. *F*: mean NO-induced E_{Cl} shifts recorded from multiple cells showing that blockade of the activity of vacuolar H^+-ATPase diminished NO-mediated cytosolic Cl^- elevation. *$P < 0.05$; **$P < 0.01$.

crine cells, depolarization induced by high external K^+ elicits a decrease in cytosolic pH (E. McMains and E. Gleason, unpublished observations). Analysis of the pH-altering abilities of more physiological depolarizing stimuli in our cells and their influence on cytosolic chloride levels could be enlightening. It is important to note, however, that any stimulus that elevates cytosolic Ca^{2+} levels could enhance plasma membrane Ca^{2+}-ATPase activity as well as NO production, rendering the interpretation of any results more complicated.

Amiloride-sensitive NHEs are the main mechanism responsible for actively regulating cytosolic pH in neurons in response to acid loads (for a review, see Chesler 2003). Blockade of NHEs with amiloride or its derivatives has been shown to result in a decrease in cytosolic pH in a number of neuronal cell types (Bonnet and Wiemann 1999; Dietrich and Morad 2010). Here, we show that amiloride lowers cytosolic pH in retinal amacrine cells as well, indicating that at rest, amiloride-sensitive NHEs are actively transporting H^+ out of the cytosol. We also show that the acidification produced by amiloride is within the physiological buffering range of amacrine cells because the pH change is transient and recovers to near resting levels within 10 s.

As demonstrated in the RESULTS, a drawback to using amiloride to block NHEs is that it can interfere with other mechanisms involving Na^+ transport, such as endothelial Na^+ channels, acid-sensing channels, and the Na^+/Ca^{2+} exchanger (Frelin et al. 1988). We have no indication that either endothelial Na^+ channels or acid-sensing channels are expressed in amacrine cells, but if any of these mechanisms were active and blocked by amiloride, we would expect to see a decrease in holding current at -70 mV when the reagent was applied; however, no such change in current was observed (not shown). We have previously established that the Na^+/Ca^{2+} exchanger is expressed in these cells and that the current produced by its electrogenic activity can be observed as a tail current after the

activation of voltage-gated Ca^{2+} channels (Gleason et al. 1995). Because we blocked voltage-gated Ca^{2+} channels in our ramp experiments (Fig. 2) and as far as we know we are not raising cytosolic Ca^{2+} by any other mechanism, we think it is unlikely that the Na^+/Ca^{2+} exchanger is active during these experiments. Although some caution should attend any pharmacological manipulation, in amacrine cells and under the conditions of our experiments, the NHE is the most likely target of amiloride, and the positive shift of E_{Cl} is primarily due to the resulting change in pH. What do our experiments with NO under altered pH conditions tell us about the mechanism underlying the NO-dependent release of internal Cl^- (Figs. 3 and 6)? In NH_4Cl, cytosolic pH is elevated and cytosolic Cl^- is reduced. The reduction in cytosolic Cl^- would increase the Cl^- gradient between an internal compartment and the cytosol, yet the amplitude of the NO-dependent shift in E_{Cl} is reduced by more than half. This, together with the inhibitory effects of strong pH buffering, suggests that the degree of NO-dependent acidification achieved is a determinant of the amount of Cl^- released. In amiloride, acidification of the cytosol is accompanied by an increase in cytosolic Cl^-; however, this does not result in a statistically significant alteration in the magnitude of the NO-dependent shift in E_{Cl}. A plausible interpretation of this result is that there is some upper bound on the effects of increased H^+ concentration, perhaps relating to saturation of a transport mechanism.

Although this work reveals some components of the NO-dependent release of Cl^- from internal stores, important questions remain. Chief among these are the identity of the store and the Cl^- transport mechanism(s) involved.

The best known sources of sequestered internal Cl^- are endosomal compartments, including early and late endosomes, lysosomes, and synaptic vesicles. It is well established that these compartments can contain 40–60 mM Cl^- (Faundez and Hartzell 2004). The internal Cl^- transporters that are known to

reside on endosomal membranes specifically are the CLC Cl^-/H^+ exchangers (for a review, see Jentsch 2008). Knockouts of CLC3 and CLC5 both produce defects in endosomal acidification (Gunther et al. 2003; Hara-Chikuma et al. 2005), and knockouts of ClC3 (Stobrawa et al. 2001) and CLC7 (Kornak et al. 2001) result in degeneration of the hippocampus and retina. Until recently, it was thought that the specific role of CLCs was to import Cl^- to offset the positive membrane potential established by inward H^+ pumping by the V-type H^+ pump (the shunt hypothesis). However, point mutations in CLC5 and CLC7 can convert these Cl^-/H^+ exchangers into pure Cl^- conductors, and functional analysis of these mutations indicated that it is the Cl^- and H^+ exchange activity, not just Cl^- transport, that is critical to normal endosomal function (Novarino et al. 2010; Weinert et al. 2010). Unexpectedly, CLC5 has been demonstrated to actually contribute to endosomal acidification by coupling the transport of H^+ into endosomes to the export of Cl^- (Smith and Lippiat 2010). It is tempting to consider that such a mechanism could provide the link between cytosolic pH and cytosolic Cl^-; however, although we have PCR and immunocytochemical evidence that amacrine cells express these transporters (McMains et al. 2011), the involvement of CLCs is yet to be tested experimentally.

NO and amacrine cells. Our current working model predicts that when an amacrine cell is stimulated to produce NO (via Ca^{2+}-dependent NOS activity), H^+ flux into the cytosol occurs either across the plasma membrane or out of organelles or both. The inhibitory effects of interfering with internal H^+ gradients on the NO-dependent increase in cytsolic Cl^- (Fig. 7) suggest that at least some H^+ flux from internal compartments is involved. The resulting acidification stimulates transport of Cl^- from internal compartments into the cytosol, shifting the E_{Cl} to a more positive value. Our findings from the present study indicate that the NO-dependent change in the weight or sign of GABAergic or glycinergic signaling (Hoffpauir et al. 2006) is dependent on both pH changes and Cl^- flux.

The amacrine cells in our cultures are GABAergic (Gleason et al. 1993) and express nNOS (unpublished observations). Four types of nNOS-expressing amacrine cells have been identified in the chicken retina, with inner plexiform layer lamination patterns that would suggest interactions with both the "on" and "off" pathways (Fischer and Stell 1999). NO electrode measurements near the soma of NO-producing retinal neurons have given NO concentrations in the tens to hundreds of nanomolar range (Eldred and Blute 2005), suggesting that the NO-mediated effects observed in the present and previous studies would be relevant only for NO-producing cells in the retina and their closest neighbors. We would expect that the pathway described in the present work would be especially relevant to nNOS-expressing amacrine cells with either GABA or glycine receptors in the retina.

We have postulated that the primary effect of NO would be to elevate cytosolic Cl^- postsynapticaly and change the weight or sign of GABAergic or glycinergic inputs. In this model, a nNOS-positive amacrine cell receiving a mixture of excitatory and inhibitory input would be responsible for a certain amount of inhibition onto downstream postsynaptic sites. Given enough excitation of the nNOS-positive cell, Ca^{2+} levels could increase to the level required for the activation of nNOS and production of NO, transiently switching inhibitory inputs into excitatory inputs and strengthening inhibition onto downstream targets. This scheme could be beneficial in two ways. First, it would be a way to add excitation to a circuit without having to generate additional glutamate. Second, the extent of the NO-induced synaptic switch could be spatially and temporally restricted, potentially building additional plasticity into the circuit.

Signaling in amacrine cells occurs mainly in dendrites, where synaptic inputs and outputs are often physically adjacent, implying that synaptic signaling can be highly localized. Indeed, this has been demonstrated physiologically at the feedback synapse between bipolar cells and A17 amacrine cells (Chavez et al. 2006; Hartveit 1999). The subcellular localization of nNOS in amacrine cell processes has been described in rat (Chun et al. 1999), guinea pig (Oh et al. 1999), and turtle (Cao and Eldred 2001) retinas. Intriguingly, these studies found that nNOS can be highly localized to synaptic sites in amacrine cell processes, and while it is well known that NOS can be anchored to N-methyl-D-aspartate receptors at postsynaptic sites, much of the labeling in amacrine cell processes was found at presynaptic sites. Perhaps the NO-dependent release of Cl^- from presynaptic vesicles could alter the performance of the adjacent postsynaptic sites. Further studies on the identity, location, and physiological properties of the Cl^- store will enable us to explore this possibility.

DISCLOSURES

No conflicts of interest, financial or otherwise, are declared by the author(s).

REFERENCES

Bonnet U, Wiemann M. Ammonium prepulse: effects on intracellular pH and bioelectric activity of CA3-neurones in guinea pig hippocampal slices. *Brain Res* 840: 16–22, 1999.

Bormann J, Hamill OP, Sakmann B. Mechanism of anion permeation through channels gated by glycine and γ-aminobutyric acid in mouse cultured spinal neurones. *J Physiol* 385: 243–286, 1987.

Boron WF, De Weer P. Intracellular pH transients in squid giant axons caused by CO_2, NH_3, and metabolic inhibitors. *J Gen Physiol* 67: 91–112, 1976.

Bowman EJ, Siebers A, Altendorf K. Bafilomycins: a class of inhibitors of membrane ATPases from microorganisms, animal cells, and plant cells. *Proc Natl Acad Sci USA* 85: 7972–7976, 1988.

Buckler KJ, Vaughan-Jones RD. Application of a new pH-sensitive fluoroprobe (carboxy-SNARF-1) for intracellular pH measurement in small, isolated cells. *Pflügers Arch* 417: 234–239, 1990.

Cao L, Eldred WD. Subcellular localization of neuronal nitric oxide synthase in turtle retina: electron immunocytochemistry. *Vis Neurosci* 18: 949–960, 2001.

Chavez AE, Singer JH, Diamond JS. Fast neurotransmitter release triggered by Ca influx through AMPA-type glutamate receptors. *Nature* 443: 705–708, 2006.

Chen G, Dunbar RL, Gao W, Ebner TJ. Role of calcium, glutamate neurotransmission, and nitric oxide in spreading acidification and depression in the cerebellar cortex. *J Neurosci* 21: 9877–9887, 2001.

Chun MH, Oh SJ, Kim IB, Kim KY. Light and electron microscopical analysis of nitric oxide synthase-like immunoreactive neurons in the rat retina. *Vis Neurosci* 16: 379–389, 1999.

Dietrich CJ, Morad M. Synaptic acidification enhances $GABA_A$ signaling. *J Neurosci* 30: 16044–16052, 2010.

Dixon DB, Takahashi K, Copenhagen DR. L-Glutamate suppresses HVA calcium current in catfish horizontal cells by raising intracellular proton concentration. *Neuron* 11: 267–277, 1993.

Eldred WD, Blute TA. Imaging of nitric oxide in the retina. *Vision Res* 45: 3469–3486, 2005.

Farrant M, Kaila K. The cellular, molecular and ionic basis of GABA$_A$ receptor signalling. *Prog Brain Res* 160: 59–87, 2007.

Faundez V, Hartzell HC. Intracellular chloride channels: determinants of function in the endosomal pathway. *Sci STKE* 2004: re8, 2004.

Fischer AJ, Stell WK. Nitric oxide synthase-containing cells in the retina, pigmented epithelium, choroid, and sclera of the chick eye. *J Comp Neurol* 405: 1–14, 1999.

Fisher JL. Amiloride inhibition of γ-aminobutyric acid$_A$ receptors depends upon the alpha subunit subtype. *Mol Pharmacol* 61: 1322–1328, 2002.

Foldy C, Lee SH, Morgan RJ, Soltesz I. Regulation of fast-spiking basket cell synapses by the chloride channel ClC-2. *Nat Neurosci* 13: 1047–1049, 2010.

Forgac M. The vacuolar H$^+$-ATPase of clathrin-coated vesicles is reversibly inhibited by *S*-nitrosoglutathione. *J Biol Chem* 274: 1301–1305, 1999.

Frelin C, Barbry P, Vigne P, Chassande O, Cragoe EJ Jr, Lazdunski M. Amiloride and its analogs as tools to inhibit Na$^+$ transport via the Na$^+$ channel, the Na$^+$/H$^+$ antiport and the Na$^+$/Ca^{2+} exchanger. *Biochimie* 70: 1285–1290, 1988.

Gleason E, Borges S, Wilson M. Electrogenic Na-Ca exchange clears Ca^{2+} loads from retinal amacrine cells in culture. *J Neurosci* 15: 3612–3621, 1995.

Gleason E, Borges S, Wilson M. Synaptic transmission between pairs of retinal amacrine cells in culture. *J Neurosci* 13: 2359–2370, 1993.

Gunther W, Piwon N, Jentsch TJ. The ClC-5 chloride channel knock-out mouse–an animal model for Dent's disease. *Pflügers Arch* 445: 456–462, 2003.

Hara-Chikuma M, Yang B, Sonawane ND, Sasaki S, Uchida S, Verkman AS. ClC-3 chloride channels facilitate endosomal acidification and chloride accumulation. *J Biol Chem* 280: 1241–1247, 2005.

Hartveit E. Reciprocal synaptic interactions between rod bipolar cells and amacrine cells in the rat retina. *J Neurophysiol* 81: 2923–2936, 1999.

Hoffpauir B, McMains E, Gleason E. Nitric oxide transiently converts synaptic inhibition to excitation in retinal amacrine cells. *J Neurophysiol* 95: 2866–2877, 2006.

Hoffpauir BK, Gleason EL. Activation of mGluR5 modulates GABA$_A$ receptor function in retinal amacrine cells. *J Neurophysiol* 88: 1766–1776, 2002.

Ito N, Bartunek J, Spitzer KW, Lorell BH. Effects of the nitric oxide donor sodium nitroprusside on intracellular pH and contraction in hypertrophied myocytes. *Circulation* 95: 2303–2311, 1997.

Kim Y, Trussell LO. Ion channels generating complex spikes in cartwheel cells of the dorsal cochlear nucleus. *J Neurophysiol* 97: 1705–1725, 2007.

Kim Y, Trussell LO. Negative shift in the glycine reversal potential mediated by a Ca^{2+}- and pH-dependent mechanism in interneurons. *J Neurosci* 29: 11495–11510, 2009.

Kornak U, Kasper D, Bosl MR, Kaiser E, Schweizer M, Schulz A, Friedrich W, Delling G, Jentsch TJ. Loss of the ClC-7 chloride channel leads to osteopetrosis in mice and man. *Cell* 104: 205–215, 2001.

McMains E, Krishnan V, Prasad S, Gleason E. Expression and localization of CLC chloride transport proteins in the avian retina. *PLos One* 6: e17647, 2011.

Medler K, Gleason EL. Mitochondrial Ca^{2+} buffering regulates synaptic transmission between retinal amacrine cells. *J Neurophysiol* 87: 1426–1439, 2002.

Mellman I. The importance of being acid: the role of acidification in intracellular membrane traffic. *J Exp Biol* 172: 39–45, 1992.

Nemargut JP, Wang GY. Inhibition of nitric oxide synthase desensitizes retinal ganglion cells to light by diminishing their excitatory synaptic currents under light adaptation. *Vision Res* 49: 2936–2947, 2009.

Novarino G, Weinert S, Rickheit G, Jentsch TJ. Endosomal chloride-proton exchange rather than chloride conductance is crucial for renal endocytosis. *Science* 328: 1398–1401, 2010.

Oh SJ, Kim HI, Kim IB, Kim KY, Huh W, Chung JW, Chun MH. Morphology and synaptic connectivity of nitric oxide synthase-immunoreactive neurons in the guinea pig retina. *Cell Tissue Res* 297: 397–408, 1999.

Pang JJ, Gao F, Wu SM. Light responses and morphology of bNOS-immunoreactive neurons in the mouse retina. *J Comp Neurol* 518: 2456–2474, 2010.

Smith AJ, Lippiat JD. Direct endosomal acidification by the outwardly rectifying CLC-5 Cl$^-$/H$^+$ exchanger. *J Physiol* 588: 2033–2045, 2010.

Sonawane ND, Verkman AS. Determinants of [Cl$^-$] in recycling and late endosomes and Golgi complex measured using fluorescent ligands. *J Cell Biol* 160: 1129–1138, 2003.

Staley KJ, Soldo BL, Proctor WR. Ionic mechanisms of neuronal excitation by inhibitory GABA$_A$ receptors. *Science* 269: 977–981, 1995.

Stobrawa SM, Breiderhoff T, Takamori S, Engel D, Schweizer M, Zdebik AA, Bosl MR, Ruether K, Jahn H, Draguhn A, Jahn R, Jentsch TJ. Disruption of ClC-3, a chloride channel expressed on synaptic vesicles, leads to a loss of the hippocampus. *Neuron* 29: 185–196, 2001.

Trenholm S, Baldridge WH. The effect of aminosulfonate buffers on the light responses and intracellular pH of goldfish retinal horizontal cells. *J Neurochem* 115: 102–111, 2010.

Vincent AM, TenBroeke M, Maiese K. Neuronal intracellular pH directly mediates nitric oxide-induced programmed cell death. *J Neurobiol* 40: 171–184, 1999.

Wang GY, Liets LC, Chalupa LM. Nitric oxide differentially modulates ON and OFF responses of retinal ganglion cells. *J Neurophysiol* 90: 1304–1313, 2003.

Wang GY, van der List DA, Nemargut JP, Coombs JL, Chalupa LM. The sensitivity of light-evoked responses of retinal ganglion cells is decreased in nitric oxide synthase gene knockout mice. *J Vis* 7: 7 1–13, 2007.

Weinert S, Jabs S, Supanchart C, Schweizer M, Gimber N, Richter M, Rademann J, Stauber T, Kornak U, Jentsch TJ. Lysosomal pathology and osteopetrosis upon loss of H$^+$-driven lysosomal Cl$^-$ accumulation. *Science* 328: 1401–1403, 2010.

Williams JR, Payne JA. Cation transport by the neuronal K$^+$-Cl$^-$ cotransporter KCC2: thermodynamics and kinetics of alternate transport modes. *Am J Physiol Cell Physiol* 287: C919–C931, 2004.